Available online at www.sciencedirect.com

ScienceDirect

Procedia Manufacturing 50 (2020) 11–16

Procedia MANUFACTURING

www.elsevier.com/locate/procedia

18th International Conference Metal Forming 2020

On the manufacturing of highly-customized near net-shape medical implants using magnesium alloy sheet

Joan Castells[a], Pasquale Guiglielmi[b], Ines Ferrer[a], Gabriel Centeno[c], Gianfranco Palumbo[b], M. Beatriz Silva[d], M. Luisa Garcia-Romeu[a,*]

[a]Departament d'Enginyeria Mecànica i de la Construcció Industrial, Escola Politècnica Superior, C/ M. Aurèlia Capmany, 17003, Girona, Spain
[b]Dipartimento di Ingegneria Meccanica, Matematica e Management, Politecnico di Bari, Viale Japigia 182, 70126 Bari, Italy
[c]Department of Mechanical and Manufacturing Engineering, University of Seville, Camino de los Descubrimientos s/n, 41092 Seville, Spain
[d]IDMEC, Instituto Superior Técnico, Universidade de Lisboa, Av. Rovisco Pais, 1049-001 Lisboa, Portugal

* Corresponding author. Tel.: -+34+972418265; fax: ++34-972419800. *E-mail address:* mluisa.gromeu@udg.edu

Abstract

The purpose of this work is defining a global methodology framework for the manufacturing of medical implants using Mg alloys by Incremental Forming process from the results attained by the authors in this field.
The methodology proposed considers two main steps, an indispensable related to material characterization that includes from the classical and mechanical to spifability testing and it includes numerical simulations. And another one related mainly to implant forming taking into account the best process parameters from the analysis carried out in the previous step. As newness, two variants of the incremental forming process, Single (SPIF) and Two-Point (TPIF) Incremental Forming, are used for the same magnesium implant geometry. Different outputs variables, mainly: Ra, Shape accuracy and Thicknesses, besides Force and Temperature were analysed for comparison purposes.

Keywords: Incremental Sheet Forming, Implants, Magnesium alloys

1. Introduction

Magnesium (Mg) alloys are attractive materials to be investigated for prostheses manufacturing, since Mg properties in terms of density, fracture toughness, elastic modulus and compressive yield strength are more similar to that of natural bones than the other metallic materials commonly used for implants, such as titanium alloys and stainless steels. Moreover, Mg can be found as a natural ion in the human body and it is a biocompatible and biodegradable metal [1]. The most important issue to be solved for forming Mg alloys is the poor formability at room temperature due to an hexagonal close-packed (HCP) crystalline structure, which restricts slip to the basal planes. In consequence, in order to produce complex shaped parts, such as human bones, a viable solution is to process the Mg alloy at higher temperatures (200÷300 °C) since additional sliding planes are activated increasing the ductility and lowering the yield stress for better forming. Several studies on Mg AZ31 alloy [2-4] have been done proving the improvement of the formability with the temperature.

A suitable forming technique that allows the previous phenomenon is Incremental Sheet Forming. Incremental Sheet Forming (ISF) represents a flexible technology for producing complex and unique components, which is well suited for small-scale production or prototyping, such as in aerospace and medical industries. In fact, for small batches, ISF needs minimal initial costs when compared to

10.1016/j.promfg.2020.08.003

conventional sheet forming processes such as stamping and deep drawing. ISF allows the forming of the sheets with minimal preparation time and manual processing, using conventional computer numerical control (CNC) machines, resulting in high flexibility and low tooling costs.

Historically, the approaches for manufacturing customized medical implants using ISF concentrated on the utilization of titanium sheet for obtaining prostheses in different body zones: mainly for cranial and facial [5-8], knee [9] or more recently clavicle [10]. Some other studies focused on the production of these medical components made of biocompatible polymer also for the cranial region (as Polyethylene (PE), Polycaprolactone (PCL) or Ultrahigh Molecular Weight Polyethylene, UHMWPE) via Single-Point Incremental Forming (SPIF), but also using partial or total dies via Two-Point Incremental forming (TPIF) [11]. If the focus is moved to the existing works on magnesium, which is an attractive solution for removable prosthesis, a lack of them is noticed, where a faint first attempt in [12] can be found, where the combination of SPIF and Electrospinning process was proposed as a possible method to manufacture medical prostheses made of a Mg alloy substrate coated by a thin layer of PCL.

The aim of this work is to sum up the first attempts performed by the authors for establishing a global methodology for the manufacturing of medical implants using Mg alloys in combination with ISF technologies. These attempts included the independent characterization of the sheet material, experimental testing in ISF considering a wide range of process parameters, numerical simulations of the process, etc., for finally assessing the optimal process conditions to produce different kind of implants. In this general framework, it will be also presented results regarding a case of removal prosthesis in a facial zone formed by ISF on Mg alloy.

2. Global methodology for the manufacturing of medical implants

Ambrogio et al. [13] in 2005 carried out the first approach to the manufacturing of a medical implant by SPIF. Forming a customized ankle support by Deep Drawing Quality (DDQ) steel through a complete reverse engineer cycle. This reverse engineer cycle was the framework under the prosthesis was manufactured and which involved starting with the acquisition of the patient's geometry to ensure an appropriate matching between the manufactured part and the patient's body.

Already in 2017, Centeno et al. [14] proposed a functional methodology to produce cranial prostheses in polymeric sheet. In their methodology, they proposed two-branch flowchart. Patient's Computerized Axial Tomography (CAT) is also the starting point, but whereas one branch mainly coincides with the steps defined in [13]: CAD/CAM processing, NC program generation and IS Forming; a second branch is added in order to take into account the material properties (from material and spifability characterization) and, failure and strain analysis in order to carry our a more appropriate material and process parameters selection.

In this paper, the methodology framework keeps the two-branches approach from [Centeno] but particularizing it for AZ31B-H24 Magnesium alloy. It is summarized in Fig. 1, where one can recognized the two lines: the material characterization and the implant forming that will be explained next.

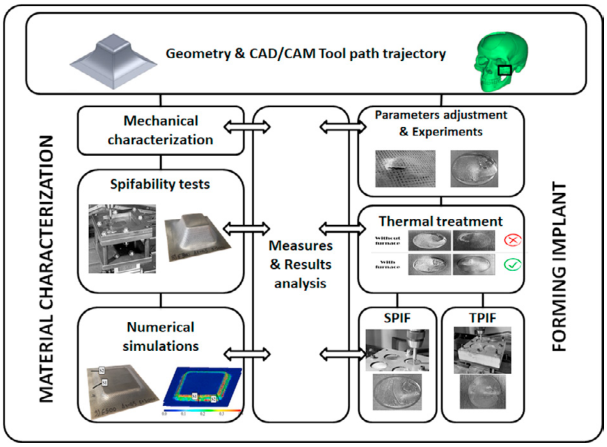

Fig. 1. Global methodology.

2.1. Geometries and tool path generation

Material characterization and implant forming lines do not share the same geometry, for the first case, a pyramidal frustum with circular generatrix for formability testing was used, Fig. 2a. Which means that there is a variable wall angle at each depth increment. The length of the edges of the pyramid was 105 mm, the initial wall angle was 45° and the generatrix radius was set to 80 mm. For implant forming, in this work a zygomatic bone (cheek bone) was chosen, Fig. 2b.

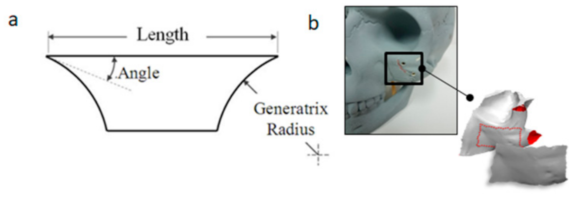

Fig. 2. (a) Pyramidal frustum (b) cheekbone geometry.

Tool path generation is a step that cannot be avoided and, in this work was done by CAM software for both geometries. For the first branch, it starts from the definition of CAD geometry and in the second, from the scanned cheekbone from a real skull processed to obtain a final CAD implant geometry.

2.2. Material Characterization: Spifability tests and Numerical Simulations

As it has been mentioned, the Magnesium alloy was AZ31B-H24 and all experimental testing was conducted using sheets of 1 mm thickness. The mechanical tests at different temperatures and, the determination of its chemical composition were done under a classical approach.

SPIF tests (frustum geometry) varying different process parameters were carried out in order to obtain the strain distribution and the FFLs. They were carried out on a Kondia® HS1000 3-axis milling machine equipped with Fidia® numerical control on flat sheets of 150 mm × 150 mm. Lubricant Houghton TD-52 minimized friction effects. Spindle Speed (2318÷5682 RPM), Step Down (0.1÷0.6 mm) and Feed Rate (232÷568 mm/min) were varied but punch diameter was kept constant (10 mm). Before each test, 3 mm circle grid was marked on the surface of the sheet. Principal strains (ε_1, ε_2) were measured by means of circle grid analysis, using the Grid Pattern Analyzer (GPA) software along three different sections of the specimen. With the thickness measurements of the specimens after fracture at several places along the crack and calculating the respective major strain by volume constancy (the average minor strain along the fracture line was considered), FFLs were obtained. The material temperature variation was also monitored with the thermographic camera IRBIS ImageIR 3300.

Regarding preliminary SPIF numerical simulations using DEFORM™-3D, they were done in order to assess the stress/strain leading to failure within the material FLD. Moreover, they were a kind of previous validation step for considering the possibility of carrying out SPIF simulations of the implant geometry.

The response in terms of principal strains of a preliminary simulation considering the flow curve of the material at a specific temperature coinciding with the maximum one register experimentally using thermography was evaluated. Details regarding the numerical model defined can be in [15].

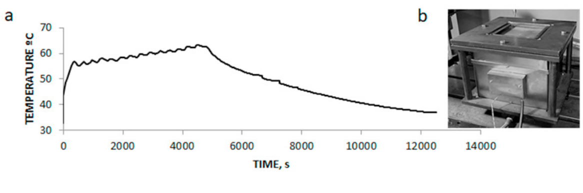

Fig. 3. Heat treatment of the undeformed sheet (b) furnace equipment.

2.3. Implant forming

SPIF machine for implant forming was the same use in previous section. Since the dimensions of the implants were small compared to the geometry considered for the formability tests, a set of preliminary screening experiments were performed in order to close the process window for process parameters determination and avoid premature ruptures of the sheets. The rupture was occurred in the last part of the forming process (at about 0.2 mm from the end)

The main results from those were: i) for avoiding excessive bending effects a tool with a diameter equal to 4mm was adopted to perform all experimental tests in addition to use a customized backing plate that allow to form 4 pieces in a sheet. ii) Increase the temperature to improve the formability of the alloy investigated during the forming process (the maximum reached temperature in some of them was around 60°C) reducing feed rate and also increasing spindle speed. The low value of temperature achieved during all test previously performed motivated the adoption of a furnace initially during the forming process. At the end, it was only used to perform a previous heating of the sheet. The thermal cycle performed (shown in Fig.3) consists of a heating phase equal to 400s up to an average temperature of 60°C, followed by 90 minutes of maintenance and then cooled in the same furnace.

In the experimentation, the three more influent process parameters have been varied: step down (Δz), feed rate (f_r) and spindle speed (S). To evaluate their best conditions, the experimental tests to be performed was obtained by adopting the Central Composite Design (CCD) method accordance with process parameters values of Table 1 with a factor α equal to 1,5. Thus, the final spindle speed range is between 3.333-6.666 rpm, step down is between 0,027-0,077mm and feed rate is between 520-200mm/min.

Table 1. Experimental values for test design.

	f_r *(mm/s)*	S *(rpm)*	Δz *(mm)*
Min	120	2500	0.015
Max	600	7500	0.090

Although in a general sense there exist few works that uses two-point incremental forming (TPIF) to form metal implants, the results of an attempt is going to be presented in this work. It was expecting to improve and ensure an appropriate geometric accuracy. A four machined cavity of the implant was done in a resin material block.

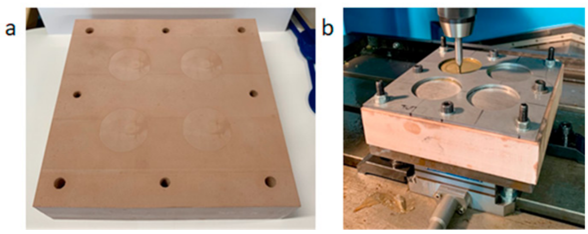

Fig. 4. (a) Four cavities machined die (b) TPIF set.

However, at the end, from all the results, the best and the worst conditions were selected to make the comparison between SPIF and TPIF geometry (see them in Table 2).

Table 2. Experimental values for test design.

	Exp	f_r *(mm/min)*	S *(rpm)*	Δz *(mm)*
SPIF	1	520	3333	0.077
	2	360	5000	0.015
TPIF	1	520	3333	0.077
	2	360	5000	0.015

2.3. Measurements

Different outputs variables roughness (R_a), shape accuracy (SA) and thicknesses (t) were selected and to analyze ISF processes. Maximum Force (F) and Temperature (T) were also recorded.

In order to evaluate the fit of the prosthesis obtained during the deformation process with the theoretical prosthesis, a measurement of the longitudinal profile was performed using the Mitutoyo coordinate machine model Crysta-Apex C544, Fig.5a This procedure resulted in a set of points treated for comparison purpose between the theoretical profile curve with the experimental obtained. In order to better overlap the two curves when calculating the deviation, the maximum height of each curve was taken as a zero reference. Because the measurement made with the coordinate machine is longer than the actual curve, the excess points on the experimental curve have been removed so that we have the same length on both curves. Then, for each point we have on the horizontal axis of the graph, we calculated its vertical difference between the two curves. These values are summed up so that the higher this value, the less accurate we are. Since it doesn't make much sense for us to talk about accuracy the higher the value of the smaller total sum is the accuracy, the inverse of that sum has been used as an index SA to evaluate the accuracy of the prosthesis. A greater value of SA represents more accuracy of the experimental prosthesis towards the real prosthesis.

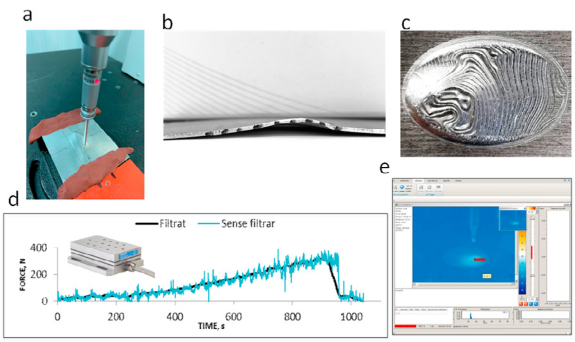

Fig. 5. (a) Profile measurement (b) Thickness section (c) Roughness (d) Force equipment (e) Temperature equipment.

Thicknesses values at several points of a cut specimen along its longitudinal axis were carried out by a caliper measurement, Fig.5b. And the roughness, also measure along the same longitudinal axis, was measured by Mitutoyo Surftest SV1000 and Surfpack-SV v1.300 software.

Forming forces were collected with a frequency of 10 values per second using the 9257B Kistler dynamometric table. Then, their magnitudes were filtered to obtain its variation over time and its maximum value. Temperature was acquired with the thermographic camera IRBIS ImageIR 3300, at a frequency of 0.1 Hz. The temperature distribution on the blank during the entire experimental tests was recorded and then processed in order to obtain the maximum temperature for each test and its variation over time. The depth achieved (Z_{max}) for each test was collected and used as formability indicator and as for simulation information.

3. Results

3.1. Characterization of the Magnesium sheet material

Chemical composition and mechanical properties of the AZ31B-H24 are shown respectively in Table 3 and Table 2.

Table 3. Mechanical properties of the Mg AZ31B workpiece material.

Testing direction	Ultimate Tensile Strenght (MPa)	Tensile Yield Strenght (MPa)
Longitudinal	283÷294	223÷232

Table 4. Chemical composition of the Mg AZ31B workpiece material.

% weight	Al	Zn	Mn	Ni	Fe
	2.5÷3.5	0.7÷1.3	0.2÷1.0	<0.005	<0.005
% weight	Cu	Si	Ca	Others	Mg
	<0.06	<0.05	<0.04	0.3	balanced

3.2. FLD and Numerical simulations of the process

Fair agreement between numerical and experimental results in terms of principal strains was obtained.

From this good results of simulation versus experimental validation, it could be considered to applied numerical simulation to predict the final strain in the implant geometry according to process parameters given. Due to moreover the zygomatic shape presents a smooth surface.

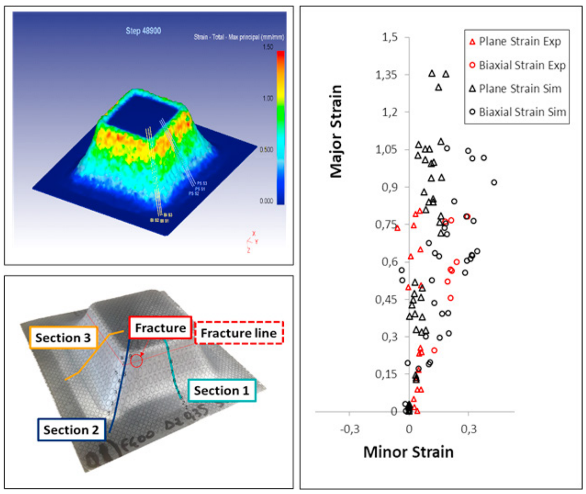

Fig. 6. Forming Limit Diagram from simulation and experimental results.

3.3. SPIF and TPIF implant results and comparison

Fig. 7 present the formed prosthesis for both manufacturing conditions and strategies. And Table 5 shows the results from the measured outputs variables.

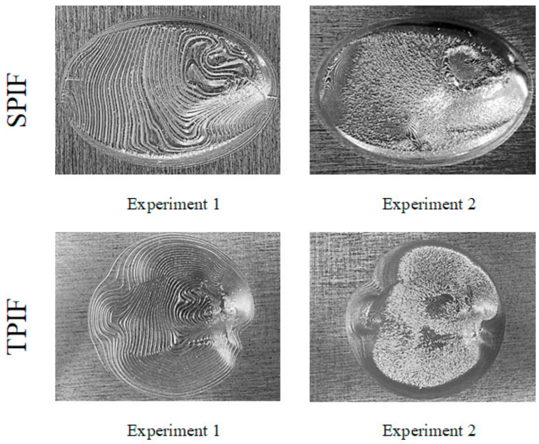

Fig. 7. Sound parts from SPIF and TPIF experiments.

As noticed in Table 5, shape accuracy (SA) is better when both step down and feed rate values are lower and spindle speed value is higher. Although the average temperature of all the experiments are quite similar each other, using these conditions, the exposure time to this temperature is longer leading to improve its formability and to adjust better to the final shape (Figure 8). Actually, using TPIF strategy the accuracy is quite better than SPIF case, from both figures and eye-naked specimen observations. Regarding to the thickness, thinning in all the cases it is quite constant less in central area of the cheekbone implant where the geometry is deeper and the deformation level is higher (Figure 8). On average, thinner prosthesis are obtained when more shape accurate are the parts (compare t values in Table 5).

Table 5. Outputs values for experiment comparison.

	Exp.	SA	t *(mm)*	Ra *(µm)*	F *(N)*	T *(ºC)*
SPIF	1	0.0168	0.8533	10,48	207,43	55,8
	2	0.0367	0.7433	4,19	309,28	55,13
TPIF	3	0.0419	0.820	13,53	271,46	51,76
	4	0.0854	0.707	6,19	268,91	61,39

Regarding to the roughness, as expected, strong visual differences are between the two steps down used in the experiments. When it is 0.077 mm the tool trajectory is strongly marked in the surface giving a roughness higher than 10µm in both manufacturing strategies. Whereas, when it is lower (0.015mm) the results are much better as expected. Comparing both strategies, it is noticed that SPIF strategy provide better roughness results than TPIF strategy, however further experiment should be done to study it.

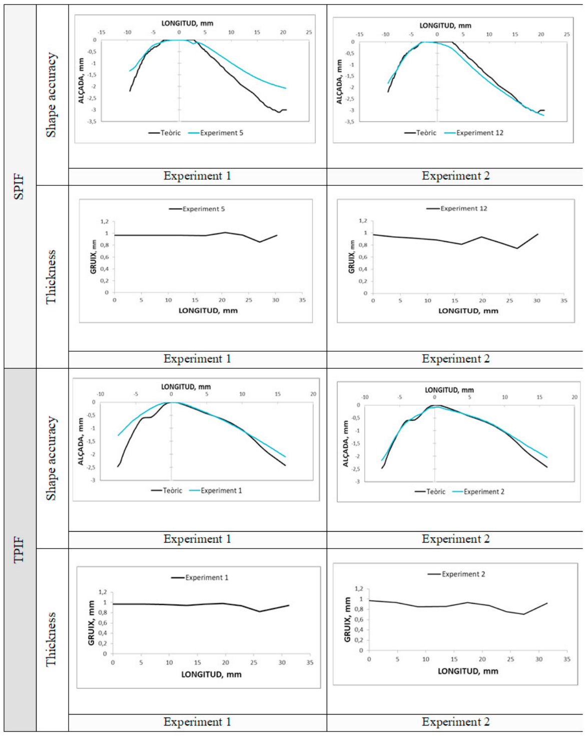

Fig. 8. Results for each output variable for SPIF and TPIF comparison.

4. Conclusions

The results provided are a compilation of new and previous outcomes from researches of the authors of the present work when using ISF processes for the manufacturing of biocompatible metal implants, in this case for a zygomatic bone from a skull in magnesium alloy.

As it could be anticipated, process parameters have a great influence on the results of the variables studied (accuracy, thickness, roughness, strength and temperature) and the expected trends have been also fulfilled. For example, how formability is improved by the increase of temperature by means of the spindle speed during ISF processes and by the pre-heat of the unformed sheets.

Therefore, the proposed global methodology has been validated for AZ31B-H24 Mg alloy and can be the framework for other magnesium alloys or biocompatible metal materials.

Acknowledgements

This research has received funding from: the University of Girona (MPCUdG2016/036), the Spanish Ministry of Education (DPI2016-77156-R) and the Catalan Agency for Management of University and Research Grants (2017-SGR-

0385); and it was also supported by the Italian Ministry of Education, University and Research under the Programme “Department of Excellence” Legge 232/2016, Grant No. CUP - D94I18000260001.

References

[1] Gupta M, Nai Mui Ling S. Magnesium, Magnesium Alloys an Magnesium Composites; 2010.

[2] Ambrogio G, Filice L, Manco GL. Warm incremental forming of magnesium alloy AZ31. CIRP Ann. - Manuf Technol 2008;57(1):257–60.

[3] Park J, Kim J, Park N, Kim Y. Study of Forming Limit for Rotational Incremental Sheet Forming of Magnesium Alloy Sheet. Metall Mater Trans A 2010;41(1):97–105.

[4] Ji YH, Park JJ. Incremental forming of free surface with magnesium alloy AZ31 sheet at warm temperatures. Trans Nonferrous Met Soc China English Ed. 2008;18(no. SPEC. ISSUE 1):165–9.

[5] Duflou JR, Lauwers B, Verbert J, Gelaude F, Tunckol Y. Medical application of single point incremental forming: Cranial plate manufacturing. Virtual Modelling and Rapid Manufacturing - Advanced Research in Virtual and Rapid Prototyping; 2005. p. 161–166.

[6] Fiorentino A, Marzi R, Ceretti E. Preliminary results on Ti incremental sheet forming (ISF) of biomedical devices: biocompatibility, surface finishing and treatment. Int J Mechatronics Manuf Syst 2012;5(1):36.

[7] Araújo R, Teixeira P, Montanari L, Reis A, Silva MB, Martins PA. Single point incremental forming of a facial implant. Prosthet Orthot Int 2014;38(5):369–78.

[8] Ambrogio G, Sgambitterra E, de Napoli L, Gagliardi F et al. Performances Analysis of Titanium Prostheses Manufactured by Superplastic Forming and Incremental Forming. Procedia Eng 2017;183:168-73.

[9] Eksteen V et al. Incremental sheet forming (ISF) in the manufacturing of titanium based plate implants in the bio-medical sector. CIE42 Proceedings; 2012. p. 16–18.

[10] Vanhove H, Carette Y, Vancleef S, Duflou JR. Production of thin Shell Clavicle Implants through Single Point Incremental Forming. Procedia Eng 2017;183:174–9.

[11] Bagudanch I, Garcia-Romeu ML, Ferrer I, Ciurana J. Customized cranial implant manufactured by Incremental Sheet Forming using a biocompatible polymer. Rapid Prototyping Journal 2017;24(1):120–9.

[12] Palumbo G, Cusanno A, Garcia Romeu ML, Bagudanch I, Contessi Negrini N, Villa T, Farè S. Single Point Incremental Forming and Electrospinning to produce biodegradable magnesium (AZ31) biomedical prostheses coated with porous PCL. Materials Today: Proceedings 2019;7:394–401.

[13] Ambrogio G, De Napoli L, Filice L, Gagliardi F, Muzzupappa M. Application of Incremental Forming process for high customised medical product manufacturing. J Mater Process Tech 2005;162–163:156–62.

[14] Centeno G, Morales-Palma D, Gonzalez-Perez-Somarriba B, Bagudanch I, Egea-Guerrero JJ, Gonzalez-Perez LM, Garcia-Romeu ML, Vallellano C. A functional methodology on the manufacturing of customized polymeric cranial prostheses from CAT using SPIF. Rapid Prototyping Journal 2017;23(4):771–80.

[15] Cusanno A, Centeno G, Garcia Romeu ML, Palumbo G. On the assessment of formability and failure of Mg sheets formed by SPIF. Numiform Conference; 2019.